

Supplementary Table S1. Summary of structural statistics^a, Related to Figures 2, 3, 4, 6 and Table 1.

	BRD3 ET	IN TP - BRD3 ET	IN CTD -BRD3 ET	NSD3 ⁽¹⁴⁸⁻¹⁸⁴⁾ - BRD3 ET
Conformationally-restricting restraints^b				
NOE based distance restraints				
Total	1277	1533	1996	1609
Intra-residue ($i = j$)	305	418	411	366
Sequential ($ i-j = 1$)	446	461	532	568
Medium range ($1 < i-j < 5$)	370	392	218	366
Long range ($ i-j \geq 5$)	156	262	835	309
Dihedral angle restraints	122	166	212	138
Hydrogen bond restraints	38	22	56	52
Total no. of conformationally-restraining restraints	1437	1721	2264	1799
No. of restraints per residue	16.3	16.0	15.3	14.3
No. of long-range restraints per residue	1.8	2.5	5.9	2.5
Residual restraint violation statistics^b				
Average no. of distance violations per structure ^c				
0.1–0.2 Å	22.3	6.7	1.2	13.2
0.2–0.5 Å	12.9	1.6 (0.45 Å) ^c	0	5.1
> 0.5 Å	0.45 (0.7Å)	0 (0.35 Å)	0 (0.14 Å)	0.1 (0.57 Å)
Average no. of dihedral angle violations per structure ^c				
1–10°	9.9	8.25	10.15	4.8
>10°	0 (8.0°)	0 (7.0°)	0.35 (11.9°)	0 (5.8°)
Model quality statistics^b			IN SH3 / ETBM - ET	
RMSD backbone atoms	0.5 Å	0.6 Å	0.5 Å / 1.1 Å	0.6 Å
RMSD heavy atoms	1.0 Å	1.1 Å	0.8 Å / 1.6 Å	1.1 Å
RMSD bond angles	1.20°	1.10°	1.20°	1.20°
RMSD bond lengths	0.019 Å	0.018 Å	0.019 Å	0.018 Å
MolProbity Ramachandran statistics ^{b,d}				
Most favored regions (%)	98.1%	97.8%	93.1%	95.4%
Allowed regions (%)	1.5%	2.2%	5.1%	4.5%
Generously allowed regions (%)	0.4%	0.0%	1.8%	0.1%
Global quality scores (Raw/Z-score) ^b				
Verify3D	0.16 / -4.82	0.18 / -4.49	0.18 / -4.49	0.39 / -1.12
ProsaII	0.68 / 0.12	0.57 / -0.33	0.47 / -0.74	0.63 / -0.08
Procheck (phi-psi) ^d	0.03 / 0.43	-0.03 / 0.20	-0.43 / -1.38	-0.24 / -0.63
Procheck (all) ^d	-0.24 / -1.42	-0.12 / -0.71	-0.56 / -3.31	-0.24 / -1.42
MolProbity clash score	9.4/-0.09	6.07 / 0.48	7.21 / 0.29	5.76 / 0.54
RPF scores ^e				
Recall/precision	0.91 / 0.88	0.89 / 0.78	0.92 / 0.94	0.97 / 0.80
F-measure/DP-score	0.89 / 0.78	0.84 / 0.71	0.93 / 0.76	0.89 / 0.89

^aStructural statistics computed for the ensemble of 20 deposited structures. ^bCalculated using PSVS 1.5 (Bhattacharya et al., 2007). Average distance violations were calculated using the sum over r^{-6} . ^cLargest violation is show in parenthesis.

^dBased on ordered residue ranges [$S(\phi) + S(\psi) > 1.8$]. ^eRPF-DP scores reflecting the goodness-of-fit of the final ensemble of structures (including disordered residues) to the NOESY data and resonance assignments (Huang et al., 2012).

Supplementary Table S2. Key intermolecular interactions between peptides and BRD3 ET in complexes^a, Related to Figure 7.

Intermolecular interactions	BRD3 ET- TP	BRD3 ET- NSD3 ₁₄₈₋₁₈₄
Hydrogen bond pairs	Gly589(O), Trp390(NE1); Ile614(O), Leu403(N); Ile614(N), Leu403(O); Glu615(OE2), Ser395(O); Ile616(O), Ile401(N); Ile616(N), Ile401(O); Phe618(N), Leu399(O); Glu619(OE2), Asn397(ND2);	Asp612(O), Lys159(N); Ile614(O), Ile157(N), Ile614(N), Ile157(O); Ile616(N), Leu155(O); Ile616(O), Leu155(N); Phe618(N), Ile153(O); Glu619(N), Ile153(O); Glu619(OE1), Ile153(N);
Salt bridges	Asp612(OD1), Arg405(NH2); Glu613(OE1), Arg402(NH1); Glu615(OE2), Arg402(NH2); Asp617(OD2), Lys400(NZ);	Glu613(OE2), Lys156(NZ); Glu615(OE2), Lys154(NZ); Asp617(OD2), Lys154(NZ);
Residues of ET forming Hydrophobic interactions	Ile584, Leu592, Val595, Val596, Ile599, Ile614, Ile616, Phe618, Leu621	Ile584, Leu592, Val595, Val596, Ile599, Ile614, Ile616, Phe618, Leu621
Residues of Peptide forming Hydrophobic interactions	Trp390, Val392, Ile401, Leu403	Ile153, Leu155, Ile157, Phe168

^aThe H-bond and salt bridges were identified using the default settings in CHIMERA (Pettersen et. al 2004) and distance measurements using PyMOL with donor-acceptor distances $\leq 3.2 \text{ \AA}$ and $\leq 4.0 \text{ \AA}$ respectively. Hydrophobic interactions were identified using PyMOL (The PyMOL Molecular Graphics System, Version 2.0 Schrodinger, LLC.).

**Supplementary Table S3. Buried surface analysis for interfaces of BRD ET complexes^a.
Related to Figure 7.**

	TP : BRD3-ET	NSD3₁₄₈₋₁₈₄ : BRD3-ET	JMJD6 : BRD3-ET PDB ID: 6BNH	NSD3₁₅₂₋₁₆₃ : BRD4-ET- PDB ID: 2NCZ
Complex	7081	9317	6677	6442
ET	6178	6035	6377	5949
Peptide	2539	4891	1900	1931
Buried surface	1635	1609	1560	1439

^aSolvent accessibility determined in units of Å² using the program *GETAREA/PyMol* (Fraczkiewicz and Braun, 1998)

Supplementary Table S4: List of Oligonucleotides, Related to STAR Methods.

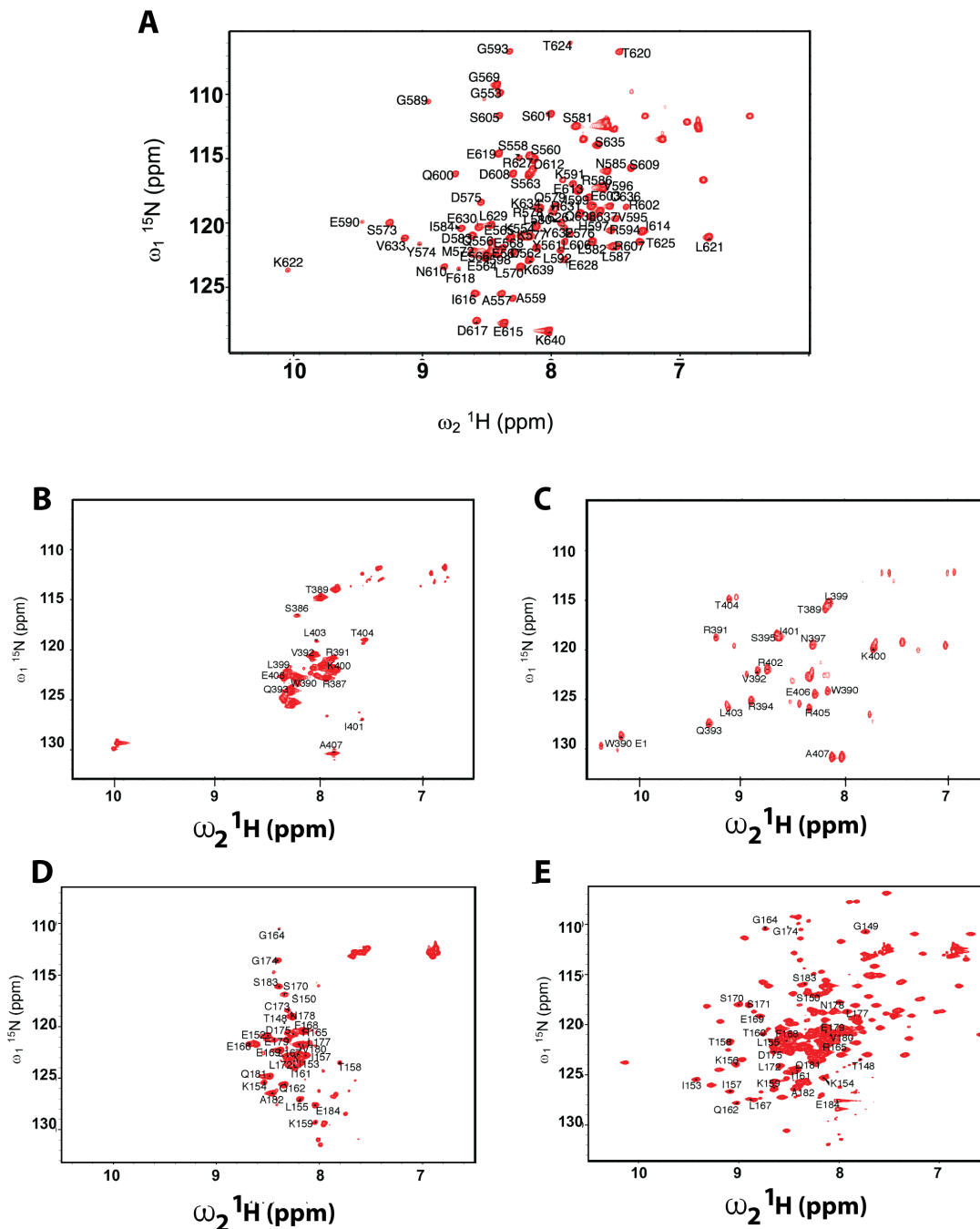
Construct	Oligonucleotide
MLV IN ₃₈₆₋₄₀₇ (IN CTD TP) duplex DNA for cloning into pGV358 vector	5' TATGAGCCGCCTGACCTGGCGCGTGCAGCGCAGCCAGAACCCGCTGAAATTCGCCCTGACCCGCGAAGCGTGCATCACGGGAGATGCA 3'
	5' CTAGTGCATCTCCCGTGATGCACGCTTCGCGGGTCAGGCGAATTTTCAGCGGGTCTGGCTGCGCTGCACGCGCCAGGTCAGGCGGCTCA 3'
Gene block synthesized for NSD3 ₁₀₀₋₂₆₃	5' GGAATTCATATGTTTCGGTGCTGTTTCGTAACCTCTCTCCGACCGACTACTACCACCTCTGAAATCCCGAACACCCGTCGCGACGAAATCCTGGAAAAACCGTCTCCGCCGACCCGCCGCCGCGCCGCTCTGTTCCGCAGACCGTTATCCCGAAAAAACCAGTTCTCTCCGAAATCAAACCTGAAAATCACCAAAACCATCCAGAACGGTCGTGAACGTTTCGAATCTTCTCTGTGCGGTGACCTGCTGAACGAAGTTCAGGCTTCTGAACACACCAAATCTAAACACGAATCTCGTAAAGAAAAACGTAAAAAATCTAACAAACACGACTCTTCTCGTTCTGAAGAACGTAATCTCACAAAATCCCGAACTGGAACCGGAAGAACAGAACCGTCCGAACGAACGTGTTGACACCGTTTCTGAAAAACCGCGTGAAGAACCGTTCTGAAAGAAGAAGCTCCGGTTCAGCCGATCCTGTCTTCTGTTCGACCACCGAAGTTTCTTATTGCATTACCGGCGATGCACTAGTCC 3'
NSD3 ₁₀₀₋₂₆₃ amplification for cloning into pSUMO vector	5' CCGGAATTCCTTCGGTGCTGTTTCGTAACCTCTCTCCG 3'
	5' CCATGAAGCTTTTAAGAAACTTCGGTGGTCGGAACAGAAGAC 3'
NSD3 ₁₄₂₋₁₆₆ duplex DNA for cloning into pSUMO vector	5' AATTCACCGTTATCCCGAAAAAACCAGTTCTCCGAAATCAAACCTGAAAATCACCAAACCATCCAGAACGGTCGTGAATAA 3'
	5' AGCTTTATTACGACCGTTCTGGATGGTTTTGGTGATTTTTCAGTTGATTTCCGGAGAACCAGTTTTCGGGATAACGGTG 3'
NSD3 ₁₄₈₋₁₈₄ amplification for cloning into pSUMO vector	5' CCGGAATTCACCGTTCTCCGAAATCAAACCTG 3'
	5' CCATGAAGCTTTTATTTCAGAAGCCTGAACTTCGTTTCAGCAG 3'
Gene block synthesized for LANA ₁₁₀₈₋₁₁₄₁ for cloning into pGV358 vector	5' GGGAAATTCATATGAATAAAGATACCTCCAAAAAAGTGCAGATGGCGCGTCTGGCGTGGGAAGCGTCCCATCCGCTGGCGGGCAATCTGCAGTCCCTCCATTGTGAAATTTAAAAAATGCATTACCGGCGATGCACTAGTCC 3'
JMJD6 ₁₋₃₃₆ amplification for cloning into pSUMO vector	5' CCGGAATTCATGAACCACAAGAGCAAGAAGCGC 3'
	5' CCATGAAGCTTTTCATGTGGACTCCTGAAGGTCAACC 3'

Supplementary Table S5: NMR samples and data used for resonance assignments, structure determination, and nuclear relaxation measurements, Related to STAR Methods.

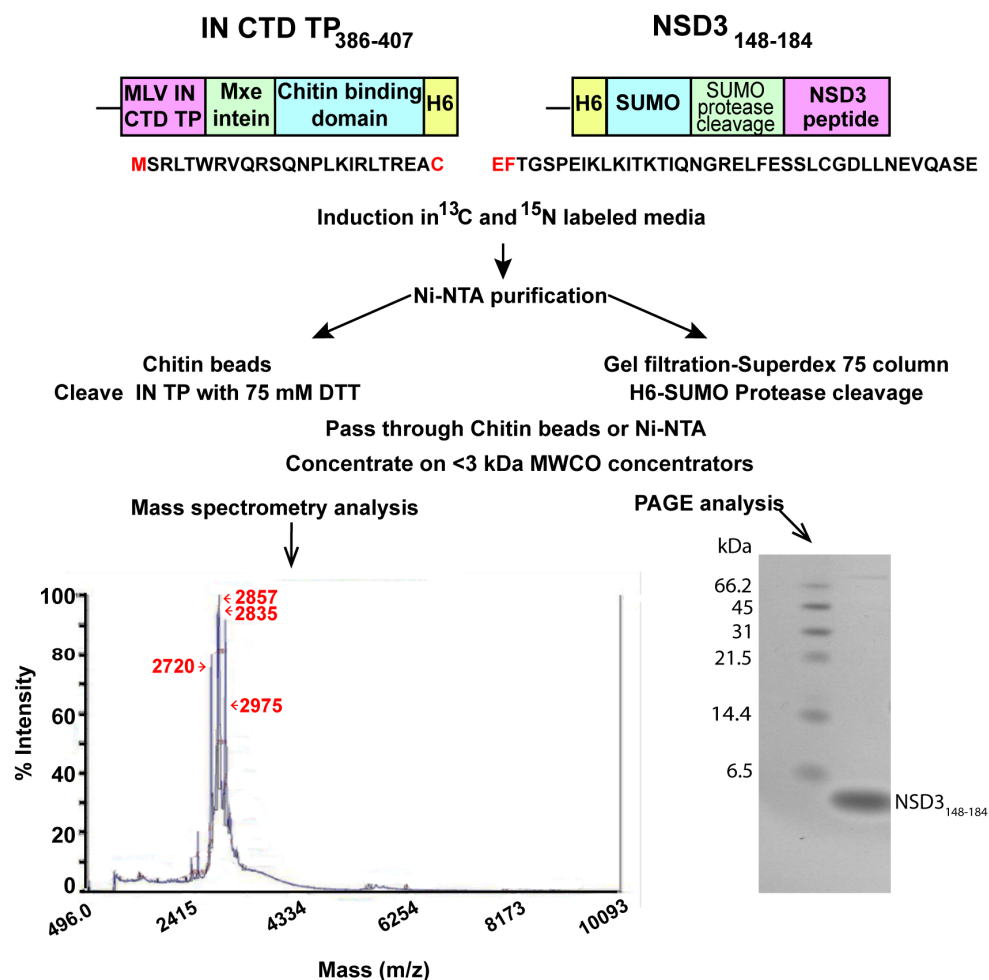
Sample	Volume (μL)	pH	NMR Tube Diameter (mm) / Probe	Field Strength	NMR Experiments
¹³ C ¹⁵ N BRD3 ET	275	7.0	4 / 5-mm CRP TXI	800 MHz	2D ¹⁵ N- ¹ H HSQC, 2D HNOE, 2D ¹³ C- ¹ H HSQC, 3D HNC0, 3D HNCA, 3D HNCACB, 3D CBCAcoNH, 3D HBHAcoNH, 3D hCCH-TOCSY, 3D ¹³ C-aromatic NOESY, 3D ¹³ C, ¹⁵ N simNOESY
¹³ C ¹⁵ N MLV IN TP	350	7.0	5 / 5-mm CRP TXI	800 MHz	2D ¹⁵ N- ¹ H HSQC, 2D HNOE, 2D ¹³ C- ¹ H HSQC, 2D ¹⁵ N- ¹ H TROSY, 3D HNCACB, 3D CBCAcoNH, 3D HBHAcoNH, 3D HNCA, 3D hCCH-TOCSY, 3D ¹³ C, ¹⁵ N simNOESY
¹³ C ¹⁵ N MLV IN TP + unlabeled BRD3 ET complex	275	7.0	4 / 5-mm CRP TXI	800 MHz	2D ¹⁵ N- ¹ H HSQC, 2D HNOE, 2D ¹³ C- ¹ H HSQC, 3D HNC0, 3D HNCA, 3D HNCACB, 3D CBCAcoNH, 3D HBHAcoNH, 3D hCCH-TOCSY, 3D ¹³ C X-filtered NOESY, 3D ¹³ C, ¹⁵ N simNOESY
¹³ C ¹⁵ N BRD3 ET + unlabeled MLV IN TP complex	275	7.0	4 / 5-mm CRP TXI	800 MHz	2D ¹⁵ N- ¹ H HSQC, 2D HNOE, 2D ¹³ C- ¹ H HSQC, 3D HNC0, 3D HNCA, 3D HNCACB, 3D CBCAcoNH, 3D HBHAcoNH, 3D hCCH-TOCSY, 3D ¹³ C X-filtered NOESY, 3D ¹³ C, ¹⁵ N simNOESY
¹³ C ¹⁵ N BRD3 ET- ¹³ C ¹⁵ N MLV IN TP complex	275	7.0	4 / 5-mm CRP TXI	800 MHz	2D ¹⁵ N- ¹ H HSQC, 2D ¹³ C- ¹ H HSQC, 3D HNC0, 3D HNCA, 3D HNCACB, 3D CBCAcoNH, 3D HBHAcoNH, 3D hCCH-TOCSY, 3D ¹³ C-aromatic NOESY, 3D ¹³ C, ¹⁵ N simNOESY
¹³ C ¹⁵ N BRD3 ET-MLV IN CTD complex	275	7.0	3 / 5-mm CRP TXI	800 MHz	2D ¹⁵ N- ¹ H HSQC, 2D ¹⁵ N- ¹ H TROSY, 2D ¹³ C- ¹ H HSQC, 3D HNC0, 3D HNCA, 3D HNcoCA, 3D HNCACB, 3D CBCAcoNH, 3D HBHAcoNH, 3D HNHA, 3D HCCH-COSY, 3D hCCH-TOCSY, 3D ¹³ C-aromatic NOESY, 3D ¹³ C, ¹⁵ N simNOESY
¹⁵ N BRD3 ET-MLV IN CTD complex	275	7.2	3 / 5-mm TCI	600 MHz	2D T1_relax, 2D T2_relax, 2D HNOE
¹³ C ¹⁵ N NSD3 ₁₄₈₋₁₈₄	40	7.0	1.7 / 5-mm TCI	600 MHz	2D ¹⁵ N- ¹ H HSQC, 2D ¹³ C- ¹ H HSQC, 2D HNOE, 3D HNC0, 3D HNCA, 3D HNCACB, 3D CBCAcoNH, 3D HBHAcoNH, 3D hCCH-TOCSY, 3D ¹³ C, ¹⁵ N simNOESY
¹³ C ¹⁵ N BRD3 ET-unlabeled NSD3 ₁₄₈₋₁₈₄	40	7.0	1.7 / 5-mm CRP TXI	800 MHz	2D ¹⁵ N- ¹ H HSQC, 2D ¹³ C- ¹ H HSQC, 2D HNOE, 3D HNC0, 3D HNCACB, 3D CBCAcoNH, 3D HBHAcoNH, 3D hCCH-TOCSY, 3D ¹³ C, ¹⁵ N simNOESY, 3D ¹³ C-aromatic NOESY, 3D ¹³ C X-filtered NOESY
¹³ C ¹⁵ N BRD3 ET- ¹³ C ¹⁵ N NSD3 ₁₄₈₋₁₈₄	275	7.0	3 / 5-mm TCI	600 MHz	2D ¹⁵ N- ¹ H HSQC, 2D ¹³ C- ¹ H HSQC, 2D HNOE, 3D HNC0, 3D HNCA, 3D HNCACB, 3D CBCAcoNH, 3D HBHAcoNH, 3D hCCH-TOCSY, 3D ¹³ C, ¹⁵ N simNOESY, 3D ¹³ C-aromatic NOESY

Solution NMR structures were determined using uniformly labeled samples of ¹³C, ¹⁵N-BRD3 ET at ~ 0.5 mM protein concentration, in buffers containing 20 mM sodium phosphate, 100 mM NaCl, 2 mM 2-mercaptoethanol at pH 7.0 (or for one sample pH 7.2). The complexes of BRD3 ET were prepared by adding the TP, MLV IN-CTD or NSD3148-184 to ET. 1D ¹⁵N T₁ and T₂ relaxation data acquired and analyzed to confirm the complex formation under the buffer conditions. These free induction decay (FID) data have been deposited in the BioMagResDatabase.

Supplementary Fig. S1. ^{15}N - ^1H]-HSQC spectrum, Related to Figures 2, 3 and 6. (A) ^{15}N - ^1H]-HSQC of BRD3 ET domain. 2D ^{15}N , ^1H]-HSQC spectrum of ^{13}C , ^{15}N BRD3 ET acquired at 25°C using 45 μL of 0.5 mM sample at pH 7.0 and 600 Hz Bruker Avance NMR spectrometer equipped with a 1.7-mm micro cryoprobe. Backbone amide ^{15}N , ^1H resonance assignments are labeled in black. (B and C). Perturbations for the ^{15}N , ^{13}C -enriched TP without and with ET domain. (B) ^{15}N - ^1H]-HSQC spectrum of unbound ^{15}N labeled MLV IN CTD TP. (C) ^{15}N - ^1H]-HSQC spectrum of ^{15}N labeled MLV IN CTD TP bound to unlabeled BRD3 ET domain. Assignments of some resonances of TP are indicated. (D and E) Perturbations for the ^{15}N , ^{13}C -enriched NSD3₁₄₈₋₁₈₄ without and with ET domain. (D) 2D ^{15}N - ^1H HSQC spectrum of ^{13}C , ^{15}N -NSD3₁₄₈₋₁₈₄. (E) ^{13}C , ^{15}N -NSD3₁₄₈₋₁₈₄- ^{13}C , ^{15}N -BRD3 ET complex. Assignments of some resonances of NSD3₁₄₈₋₁₈₄ are indicated.



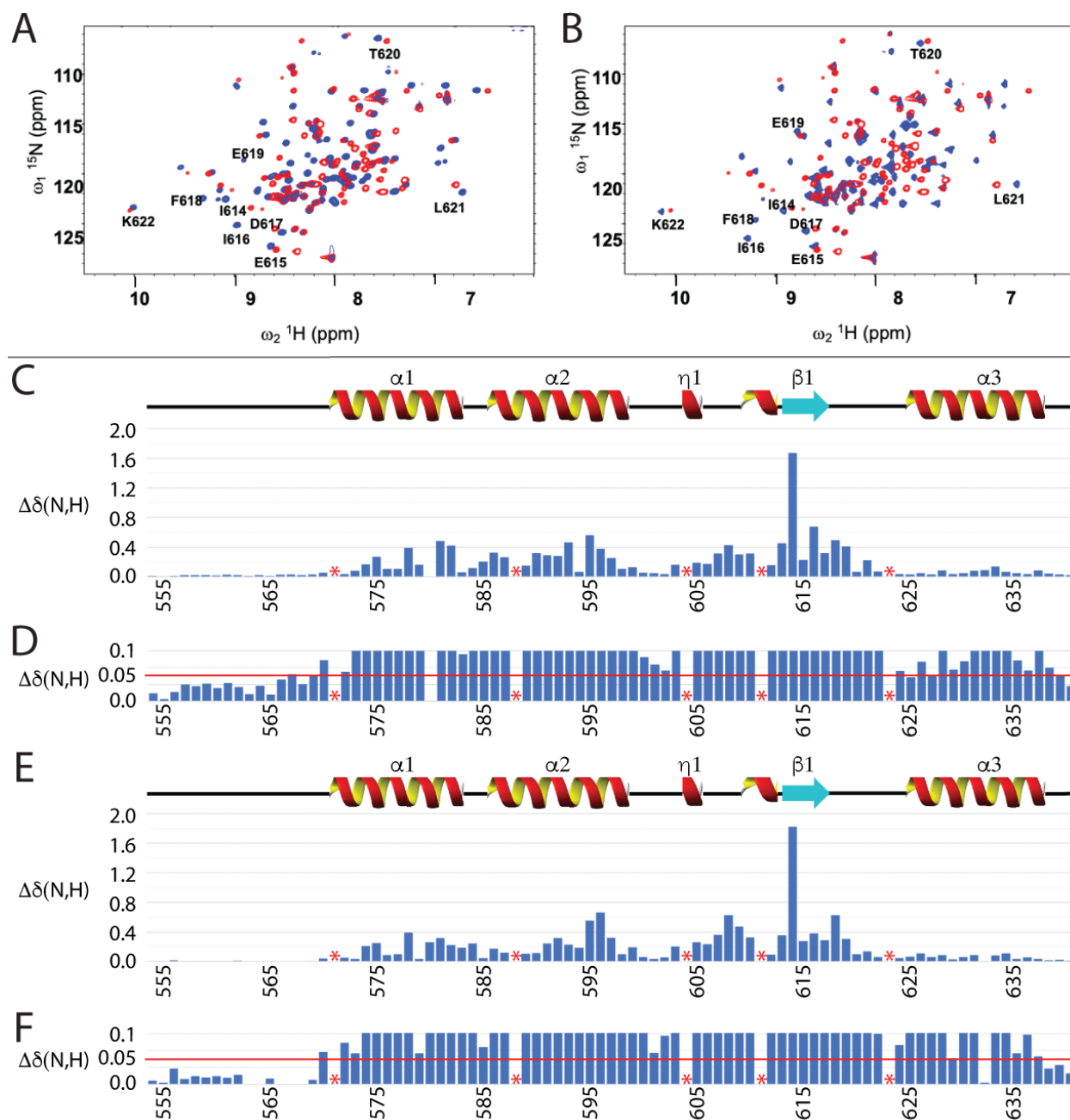
Supplementary Fig. S2. Peptide purification schematic, Related to Figures 3 and 6. Isotopically enriched peptides for NMR analyses were initially expressed as fusion proteins in *E.coli*, to facilitate cost effective rapid structure determination. The schematic of the IN CTD TP₃₈₆₋₄₀₇ chitin binding domain (CBD) fusion protein (left) and the NSD3₁₄₈₋₁₈₄-SUMO fusion protein (right) are illustrated at the top. Position of the His₆ tag (H6) is indicated. The sequences of the peptides are indicated below each construct; amino-acid residues indicated in red are not encoded by the peptides of interest. For MLV CTD IN TP₃₈₆₋₄₀₇, the C-terminal fusion of an intein-based self-cleavage system to express the peptide as a fusion protein encoded a non-native methionine at the N-terminus to initiate translation (right). The terminal Pro-408 was omitted, since prolines are incompatible with the intein self-cleavage system. Excluding the terminal proline did not affect the stability and binding efficiency of the TP construct. Purification of the peptides follow parallel protocols. On-column self-cleavage of the intein-CBD-6xHis under highly reducing conditions (Mitchell and Lorsch, 2015) following by affinity purification resulted in a greater than 90% pure, tagless peptide as assessed by mass spectrometry. Exemplary mass spectrometry of the TP₃₈₆₋₄₀₇ is shown on the left. The predicted molecular mass of the labeled peptide containing the N-terminal Met is 2830. Species smaller migrating at 2720 could result from loss of the terminal Met. Products larger at 2975 Da could result from incomplete removal of the DTT adduct after cleavage of the CBD. Using this purification strategy, we obtained highly-purified isotopically-enriched IN CTD TP with a yield of ~1.5 mgs per 1.5 liter culture. The schematic of the NSD3₁₄₈₋₁₈₄-SUMO fusion protein is shown on the right. Parallel purification involved Nickel NTA affinity column purification, S75 size exclusion chromatography, enzymatic cleavage by the SUMO-protease, and concentration. Exemplary Coomassie staining of the purified NSD3 peptide is shown on the bottom right. Molecular weight standards are as indicated.



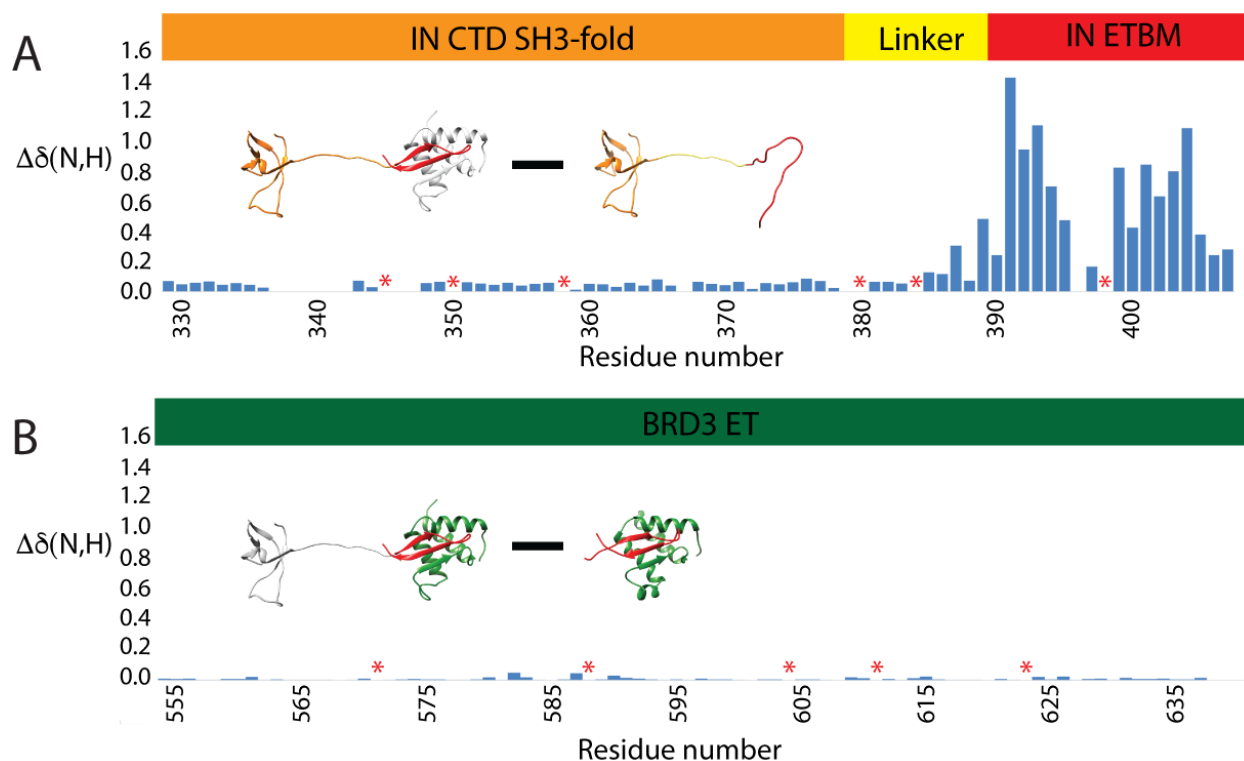
Supplementary Fig. S3. Alignment of gammaretroviral IN linker regions (top) and NSD3 (bottom) proteins, Related to Figures 4, 5 and 7. Alignments were performed using Clustal Omega (1.2.4) (Madeira et al., 2019, Sievers et al., 2011, Sievers and Higgins, 2018). Gammaretroviruses analyzed include: P10273- Feline leukemia virus, Q83379- Rat Leukemia virus, MH450110.1- Xenotropic murine leukemia virus (MLV) isolate AKR6, O39735- Friend murine leukemia virus, O41250- Rauscher murine leukemia virus, P08361- Cas-Br-E MLV, ABU54793.1- Amphotropic MLV 4070A, P03355- Moloney murine leukemia virus, P10272- Baboon endogenous virus, Q8J4V8- PERV-A, P21414- GaLV, and Q9TTC1- KoRV. M-MLV Δ 5 and Δ 20 were isolated as described (Loyola et al., 2019). NSD3 protein sequences analyzed include: F1QV68- NSD3 (zebrafish), A0A1L8H2H2- NSD3 (xenopus), E1BNH7- NSD3 (bovine), F6WYL3- NSD3 (horse), Q9BZ95-NSD3 (human), H2R3Q8- NSD3 (chimpanzee), A0A286ZK72- NSD3 (pig), E2QUJ0-NSD3 (dog), M3WJ59-NSD3 (cat), Q6P2L6- NSD3 (mouse), and D3ZK47- NSD3 (rat). Consensus sequences notations are: (*) fully conserved residue, (:) conservation between groups of strongly similar properties, and (.) conservation between groups of weakly similar properties (Gonnet et al., 1992). IN-TP and NSD3 peptide used in these studies are indicated in bold. Pro are highlighted in yellow. Conserved Trp for MLV-IN and Phe for NSD3 that form the cap to the hydrophobic network are highlighted in cyan. Position and conservation of the two beta-strands (B) of MLV IN and NSD3 interacting with the ET domain are indicated in red.

Gammaretrovirus				
FeLVa (Feline)	KAAG P TTNQDLSDS P SSDD P SRW K VQRTQ N PLKIRLSRGT-	BBB	BBBB	412
RaLV (Rat)	KAAR P EETADHN-----IA P Q T WKAQRTQ N PLKLRFSRCCS			414
XMLV (Xenotropic)	KAAT P -----PAGAA K VQ R SQ N PLKIRLTRG A P			405
MLV (Friend)	KAADTKIE-- P -----P S EST W RVQ R SQ N PLKIRLTRG T S			408
MLV (Rauscher)	KAADTRIE-- P -----P S EST W RVQ R SQ N PLKIRLTRG T S			408
MLV (CasBrE)	KAAT P -----ARTAW K VQ R SQ N PLKIRLSRE P S			405
MLV (Ampho/4070A)	KAADTESG-- P S-----S-G R T W RVQ R SQ N PLKIRLTRG S P			408
MLV (Moloney)	KAAD P GGG-- P S----- S RL T W R VQ R SQ N PL K IR L TRE A P			408
MLV Δ 5 (Moloney)	KAAD P GGG--LC-----GR K L T W R VQ R SQ N PL K IR L TRE A P			409
MLV Δ 20 (Moloney)	KAAD P G-----R K L T W R VQ R SQ N PL K IR L TRE A P			404
BaEV (Baboon)	KAAP G TP P G P -----T S SG T W R L R RS E D P L K IR L S R T--			392
PERVA (Porcine)	K P AP P -----P D SG W K A E K T E N P L K L R L H R V V P			400
GaLV (Gibbon Ape)	K P AP P S-----A P DES W E L E K T D H P L K L R I R R R R D			373
KoRVA (Koala)	K P AP P G-----A P DES W E L E K T D H P L K L R V R R R R N			373
Consensus	* *	* . . : : . * * * * : . *		
NSD3				
NSD3zebrafish	VL P PP P LL L L P SS P LL S PQ E ST I S N P I G O P V NT I IT T P			221
NSD3xenopus	P E P T S P PN L L Q A----- P PS S T-T P EQ			148
NSD3bovine	P Q P PP P ----- P PS V PQ T V I P			146
NSD3Horse	P Q P PP----- P PS V PQ T V I P			145
NDS3human	P Q P PP----- P PS V PQ T V I P			145
NSD3chimpanzee	P Q P PP----- P PS V PQ T V I P			145
NSD3pig	P Q P PP----- P PS V PQ T V I P			145
NSD3dog	P Q L PP----- P PS V PQ T V I P			145
NSD3cat	P Q P PP----- P PS V PQ T V I P			145
NSD3mouse	P Q P PP----- P PS V PQ T V I P			145
NSD3rat	P Q P PP P LL P PP----- P PP V PQ T V I P			146
Consensus			* *	
NSD3zebrafish	K K T S P E I K L K I K T Y Q NG R E L F E S S L C G D L L Q E F Q A G E D S R	BBB	BBB	263
NSD3xenopus	K K T G S P E I K L R I T K T I Q N G R E M F E S S L C G D L L H E F Q A S E M T R			190
NSD3bovine	K K T G S P E I K L K I T K T I Q N G R E L F E S S L C G D L L N E V Q A S E H T K			188
NSD3horse	K K T G S P E I K L K I T K T I Q N G R E L F E S S L C G D L L N E V Q A S E H T K			187
NDS3human	K K T G S P E I K L K I T K T I Q N G R E L F E S S L C G D L L N E V Q A S E H T K			187
NSD3chimpanzee	K K T G S P E I K L K I T K T I Q N G R E L F E S S L C G D L L N E V Q A S E H T K			187
NSD3pig	K K T G S P E I K L K I T K T I Q N G R E L F E S S L C G D L L N E V Q A S E H T K			187
NSD3dog	K K T G S P E I K L K I T K T I Q N G R E L F E S S L C G D L L N E V Q A S E H T K			187
NSD3cat	K K T G S P E I K L K I T K T I Q N G R E L F E S S L C G D L L N E V Q A S E H T K			187
NSD3mouse	K K T G S P E I K L K I T K T I Q N G R E L F E S S L C G D L L N E V Q A S E H T K			187
NSD3rat	K K T G S P E I K L K I T K T I Q N G R E L F E S S L C G D L L N E V Q A S E H L K			188
Consensus	***.*****:* ** *****:*****:*.*** ** :			

Supplementary Fig. S4. Comparison of chemical shift perturbations of BRD3 ET induced by IN TP and NSD3, Related to Figures 3 and 6. Panels A and B: HSQC of the BRD3 ET (blue) in the presence of unlabeled IN TP (panel A, red) and NSD3 (panel B, red). Chemical shift perturbations of BRD3 ET domain relative to the bound (C, D) TP and (E, F) NSD3₁₄₈₋₁₈₄ calculated using $\Delta\delta(N,H) = ((\delta N/6)^2 + (\delta H)^2)^{0.5}$ and plotted as a function of BRD3 ET sequence. Panels D and F show an expansion of the data in Panels C and E, demonstrating that most residues have $\Delta\delta(N,H)$ greater than 0.05 ppm (horizontal red lines), a typical cutoff value for unperturbed chemical shift changes on complex formation (Ma et al., 2016). Amino-acid residue positions marked with a red * correspond to Pro. Assignments of some resonances of ET are indicated. Secondary structure of BRD3 ET is shown schematically in panels C and E.



Supplementary Fig. S5. Comparison of chemical shift perturbations of backbone amides, Related to Figures 2, 3, 4 and 5. (A) Chemical shift perturbations of MLV IN CTD, in complex with BRD3 ET minus chemical shifts of apo MLV IN CTD. (B) Chemical shift perturbations of BRD3 ET, in complex with MLV IN CTD : BRD3 ET minus chemical shifts of MLV IN TP : BRD3 ET. Inset of the ribbon diagrams in color indicate the amide $^{15}\text{N},^1\text{H}$ resonances being compared while the rest is shown in gray. Residue numbers of the IN CTD and BRD3 ET domain are indicated in each panel (bottom) along with the schematic of the domains (top). Residues indicated by a red * correspond to Pro.



Supplementary Fig. S6. Comparison of chemical shift perturbations of BRD3 ET induced by LANA and JMJD6, Related to Figures 2 and 3. (A) Constructs of LANA and JMJD6. Chemical shift perturbations of BRD3 ET domain relative to the bound (B) LANA and (C) JMJD6 calculated using $\Delta\delta(N,H) = ((\delta_N/6)^2 + (\delta_H)^2)^{0.5}$ and plotted as a function of BRD3 ET sequence. Amino-acid residue positions marked with a red * correspond to Pro. The residues that were not assigned in the spectrum due to ambiguity of the assignment or missing cross peaks in the complex are included with $\Delta\delta(N,H)=0$. (D) and (E) are the perturbations mapped onto the 3D structure of BRD3 ET and IN TP (IN TP is not displayed for ease of visualization) indicating the major interactions of the peptides are in the region of ${}_{613}\text{EIEID}_{617}$ in both the complexes in addition to those shown.

